Supporting Information

Ionic Exchange of Metal-Organic Frameworks to Access Single Nickel Sites for Efficient Electroreduction of CO_2.

Changming Zhao,[†] Xinyao Dai,[†] Tao Yao,[§] Wenxing Chen[‡], Xiaoqian Wang,[†] Jing Wang,[†] Jian Yang,[†] Shiqiang Wei,[§] Yuen Wu,*[†] and Yadong Li*[‡]*

[†] Department of Chemistry, *i*ChEM (Collaborative Innovation Center of Chemistry for Energy Materials), University of Science and Technology of China, Hefei 230026, China

[‡]Department of Chemistry and Collaborative Innovation Center for Nanomaterial Science and Engineering, Tsinghua University, Beijing 100084, China

[§]Hefei National Laboratory for Physical Sciences at the Microscale, University of Science and Technology of China, Hefei, Anhui Province 230026, (China)

Table of contents

1.Material Synthesis and Characterization:

Chemicals:

Analytical grade Zinc nitrate hexahydrate ($Zn(NO_3)_2.6H_2O$), Nickel (II) nitrate hexahydrate ($Ni(NO_3)_2.6H_2O$), 2-methyl imidazole, Potassium bicarbonate ($KHCO_3$) were obtained from Shanghai Chemical Reagents, China. Nafion was acquired from Sigma-Aldrich. All of the chemicals used in this experiment were analytical grade and used without further purification. Carbon Paper (Toray) was from Alfa Aesar and ultrasonically cleaned in ethanol. Deionized (DI) water from Milli-Q System (Millipore, Billerica, MA) was used in all our experiments.

Experimental Section:

Synthesis of ZIF-8.

In a typical procedure, 0.558 g $Zn(NO_3)_2 \cdot 6H_2O$ was dissolved in 15 ml methanol, which was subsequently added into 15 ml methanol containing 0.616 g 2-methylimidazole (MeIM) under ultrasound for 10 min at room temperature. The ZIF-8 was then grown under static at 35℃ for 12 h. The as-obtained precipitates were centrifuged and washed with methanol three times and dried in vacuum at 65℃ for overnight[1].

Synthesis of Ni SAs/ N-C.

In a normal procedure, the powder of ZIF-8 (100 mg) was dispersed in n-hexane(10 ml) under ultrasound for 5 min at room temperature. After forming homogeneous solution, $Ni(NO_3)_2$ aqueous solution(100 mg ml^{-1}, 50 μL) was injected into the mixed solution slowly under ultrasound for 2 min at room temperature. Next, the mix solution was under vigorous stirring for 3 h at room temperature in order to make the salt solution be absorbed completely. Then the sample were centrifuged and dried in vacuum at 65℃ for 6 h.

The sample was placed in a tube furnace and heated to 1000 ℃(heating rate 5 ℃/min) for 2 h in a stream of Ar (10 ml/min) to yield Ni SAs/N-C. The Ni content was measured to be 1.53 wt% based on ICP-AES analysis.

Synthesis of Ni NPs/N-C.

The powder of ZIF-8 (100 mg) was dispersed in 100mg/ml $Ni(NO_3)_2$ methanol solution (10 ml) under ultrasound for 5 min at room temperature. Then, the mix solution was under vigorous stirring for 3 h at room temperature in order to make the salt methanol solution be absorbed completely. Next, the sample were centrifuged and dried in vacuum at 65℃ for 6h.

The sample was placed in a tube furnace and heated to 1000 ℃(heating rate 5 ℃/min) for 2 h in a stream of Ar (10 ml/min) to yield Ni NPs.

Characterization:

Powder X-ray diffraction patterns of samples were recorded on a Rigaku Miniflex-600 operating at 40 kV voltage and 15 mA current with CuKα radiation (λ=0.15406nm). Aberration-corrected High-angle annular dark-field scanning transmission electron microscopy (HAADF-STEM) images and the EDS of samples were performed with a JEOL JEM-2010 LaB6 high-resolution transmission electron microscope operated at 200 kV. The scanning electron microscope (SEM) was performed on JSM-6700F SEM. Thermogravimetric analyses (TG and DTA) were carried out on a TA SDT Q600 thermal analyzer heating from room temperature to 1000 °C at the rate of 5 °C min^{-1}. Elemental analysis of Ni in the solid samples was detected by inductively coupled plasma atomic emission spectrometry (Optima 7300 DV). The samples were degassed at 300 °C for 3 h. The obtained adsorption-desorption isotherms were evaluated to give the pore parameters including Brunauer-Emmett-Teller (BET) specific surface area and pore size. The pore size distribution was calculated from the HK method. These were all performed on a Micromeritics Tristar Ⅱ3020M. X-ray photoelectron spectroscopy (XPS) was collected on scanning X-ray microprobe (PHI 5000 Verasa, ULAC-PHI, Inc.) using Al Ka radiation and the C1s peak at 284.8 eV as internal standard. XAFS measurement and data analysis：XAFS spectra at the Ni K-edge was collected at BL14W1 station in Shanghai Synchrotron Radiation Facility (SSRF). The electron storage ring of SSRF was operated at 3.5 GeV with a maximum current of 250 mA. The Ni K-edge XANES data were recorded in a fluorescence mode. Ni foil, NiO were used as references. The liquid products were quantified by nuclear magnetic resonance (NMR) (Bruker AVANCE AV III 400) spectroscopy using dimethyl sulfoxide as an internal standard. During chronoamperometry, effluent gas from the cell went through the sampling loop of a gas chromatograph (shiweipx GC-7806) and was analysed in 30 min intervals to determine the concentration of gas products. The gas chromatograph was equipped with a molecular sieve TDX-01 and Al_2O_3 capillary column with Ar (Ultra high purity) flowing as a carrier gas. The separated gas products were analysed by a thermal conductivity detector (for H_2) and a flame ionization detector (for CO and hydrocarbons).

2.Electrochemical Measurements：

The experiments were performed in a gas-tight cell with two-compartments separated by an cation exchange membrane (Nafion®115, dupont). Each compartment contained 20 ml electrolyte (0.5 M $KHCO_3$ made from de-ionized water) with approximately 10 ml headspace. Pt plate was used as a counter electrode. All potentials were measured against an Ag/AgCl reference electrode (saturated KCl, obtained from Tjaida and stored in saturated KCl solution before use) and were converted to those against a reversible hydrogen electrode (RHE). In a typical prepared procedure of the working electrode, 40 μL of the homogeneous ink, which was prepared by dispersing 5 mg sample and 80 μL Nafion solution (5 wt%) in 1 mL ethanol solution, was loaded onto the two sides of a carbon fiber paper electrode with 1×1 cm^2.

During the CO_2 reduction experiments, the electrolyte in the cathodic compartment was stirred at 500 rpm. Linear sweep voltammetry (LSV) was performed with a scan rate of 10mV s^{-1} from -0.6V to -1.8V *vs.* Ag/AgCl in N_2-saturated 0.5 M $KHCO_3$ (pH=8.8) and CO_2-saturated 0.5 M $KHCO_3$(pH=7.2) as supporting electrolyte. The potentials in the study were reported versus RHE with the conversion E (*vs.* RHE) = E (*vs.* Ag/AgCl) + 0.1989 V + 0.059 × pH.

The current density was obtained by normalized with the carbon fiber paper geometric

surface area. CO_2 gas was delivered at an average rate of 10 ml/min (at room temperature and ambient pressure) and routed directly into the gas sampling loop (20 μL) of a gas chromatograph. The gas phase composition was analyzed by GC every 30 min. The separated gas products were analyzed by a thermal conductivity detector (for H_2) and a flame ionization detector (for CO). Quantification of the products was performed with the conversion factor derived from the standard calibration gases.Liquid products were analysed afterwards by quantitative NMR using dimethyl sulphoxide (DMSO) as an internal standard. Solvent presaturation technique was implemented to suppress the water peak.

Faradaic efficiency:

The faradaic efficiency **for CO production** is calculated at a given potential as follow:

$$E_F = \frac{J_{CO}}{J_{total}} = \frac{v_{CO} \times N \times F}{J_{total}}$$

J_{CO} : partial current density for CO production;

J_{total}: total current density;

N: the number of electron transferred for product formation, which is 2 for CO;

v_{CO}: the production rate of CO (measured by GC);

F: Faradaic constant, 96485 C mol^{-1};

E_F: faradaic efficiency for CO production.

Turnover Frequency (TOF, h^{-1}):

The TOF for CO was calculated as follow:

$$TOF = \frac{I_{product}/NF}{m_{cat} \times \omega / M_{Ni}} \times 3600$$

$I_{product}$: partial current for certain product, CO;

N: the number of electron transferred for product formation, which is 2 for CO;

F: Faradaic constant, 96485 C mol^{-1};

m_{cat}: catalyst mass in the electrode, g;

ω: Ni loading in the catalyst;

M_{Ni}: atomic mass of Ni, 58.69 g mol^{-1}.

3. Supporting Figures and Tables:

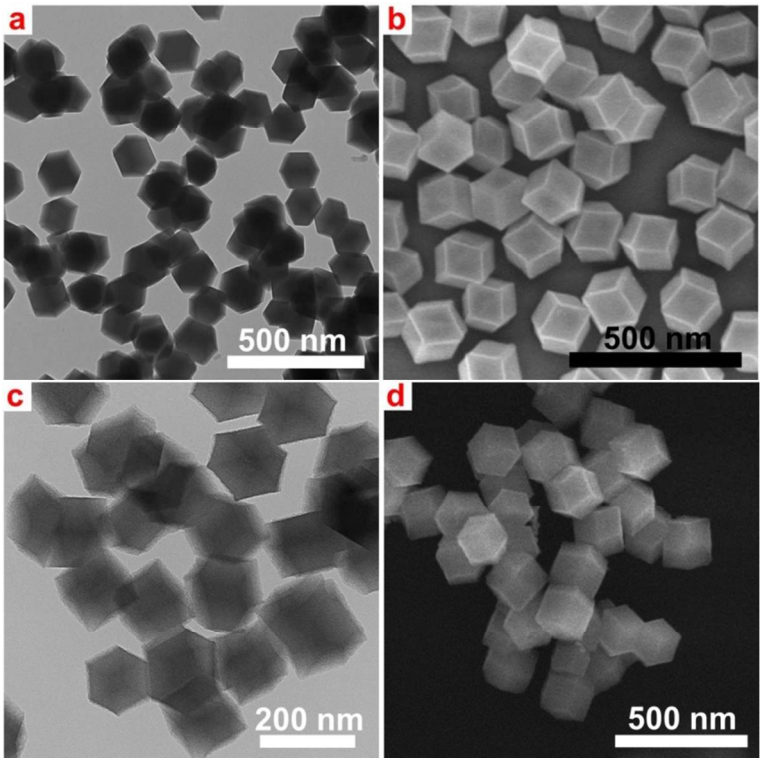

Fig. S1. (a) TEM image and (b) SEM image image of ZIF-8. (c) TEM image and (d) SEM image of pyrolyzed ZIF-8.

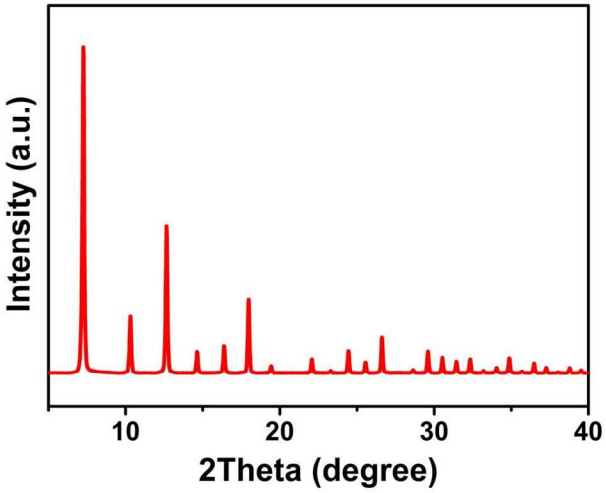

Fig. S2. XRD pattern of ZIF-8.

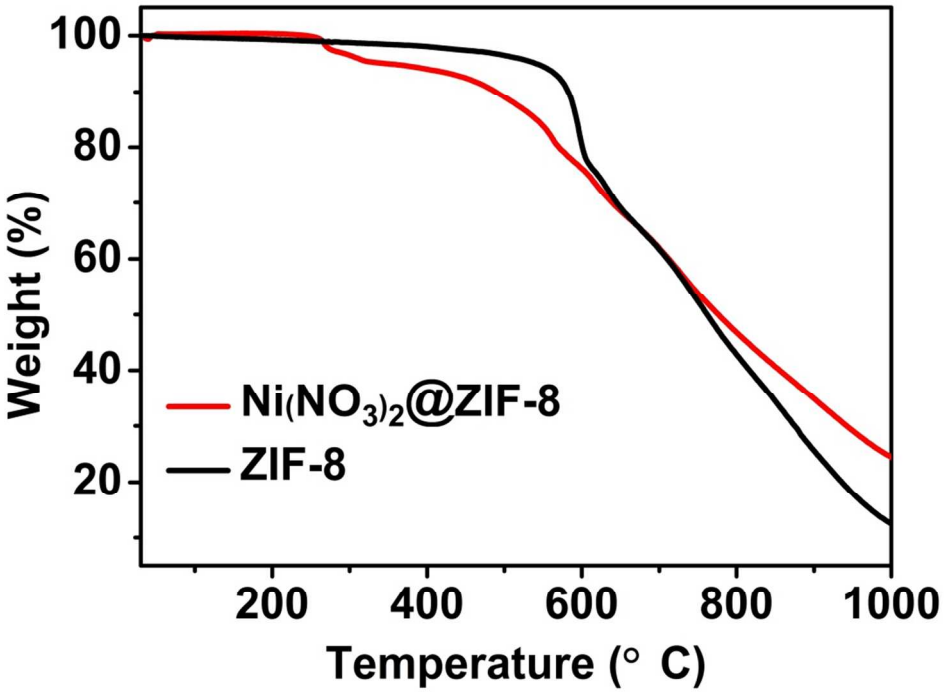

Fig. S3. TGA patterns of ZIF-8 and the composite of $Ni(NO_3)_2$ adsorbed within ZIF-8.

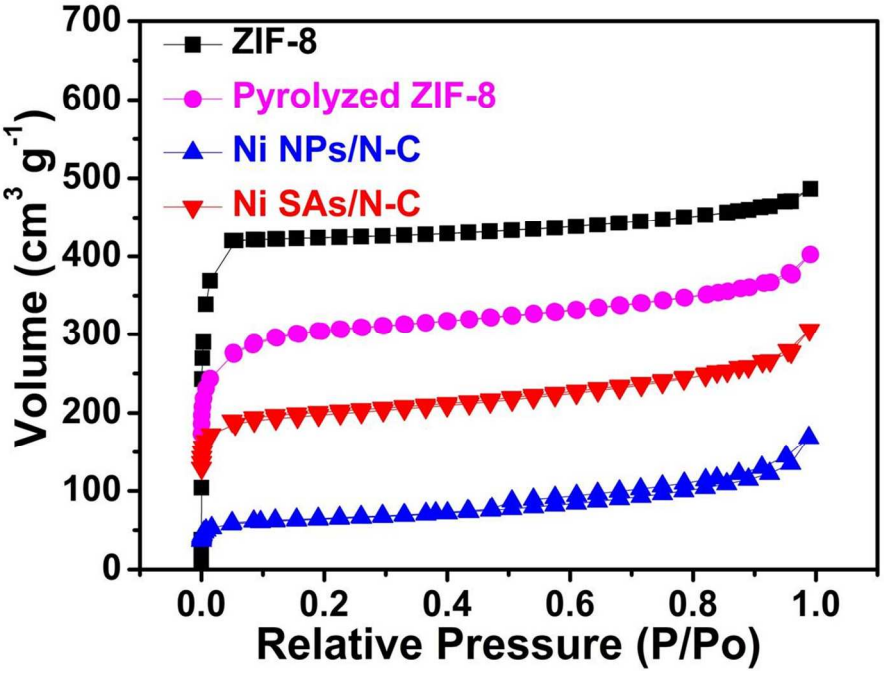

Fig. S4. N_2 adsorption and desorption isotherm for Ni SAs/N-C, Ni NPs/N-C, ZIF-8, pyrolyzed ZIF-8.

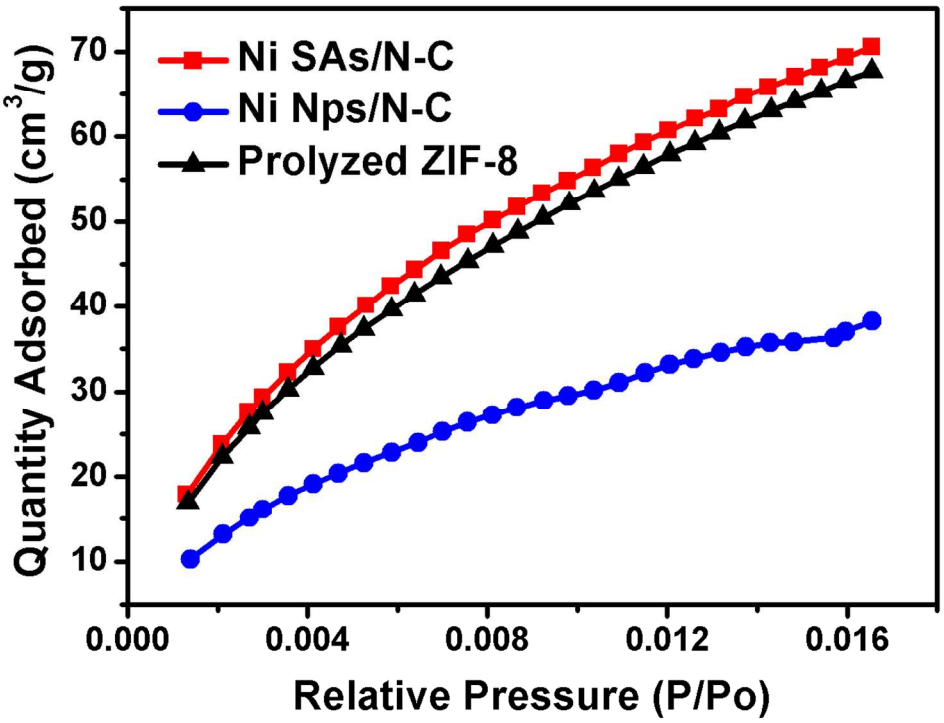

Fig. S5. CO_2 adsorption isotherms for Ni SAs/N-C, Ni NPs/N-C and pyrolyzed ZIF-8.

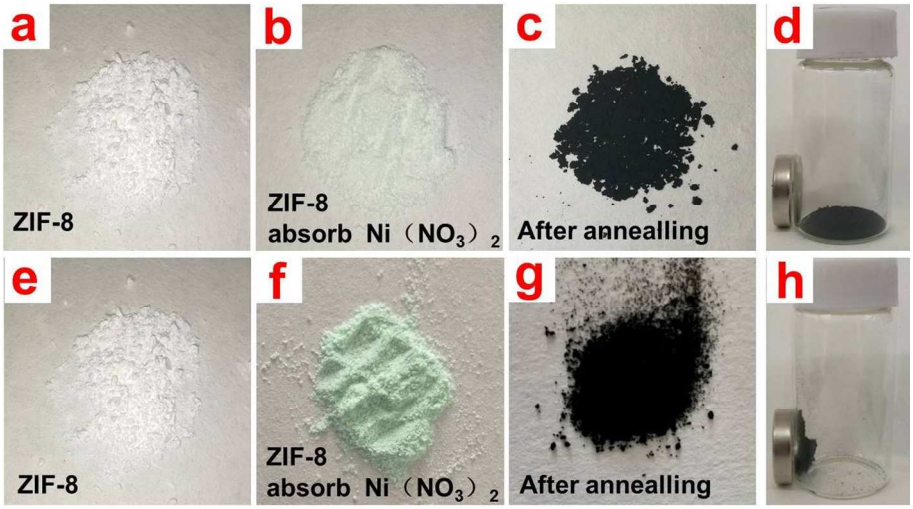

Fig. S6. (a-c) The color evolution during the preparation of Ni SAs/N-C. (e-g) The color evolution during the preparation of Ni NPs/N-C. The (d) Ni SAs/N-C, (h) Ni NPs/N-C showing different magnetic properties under the external magnet.

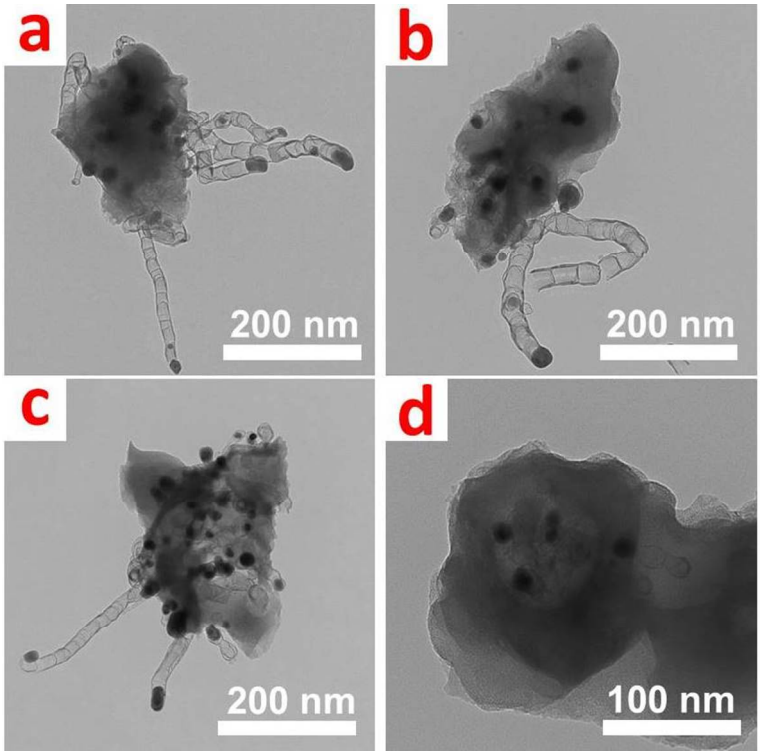

Fig. S7. The representative TEM images of Ni NPs/N-C.

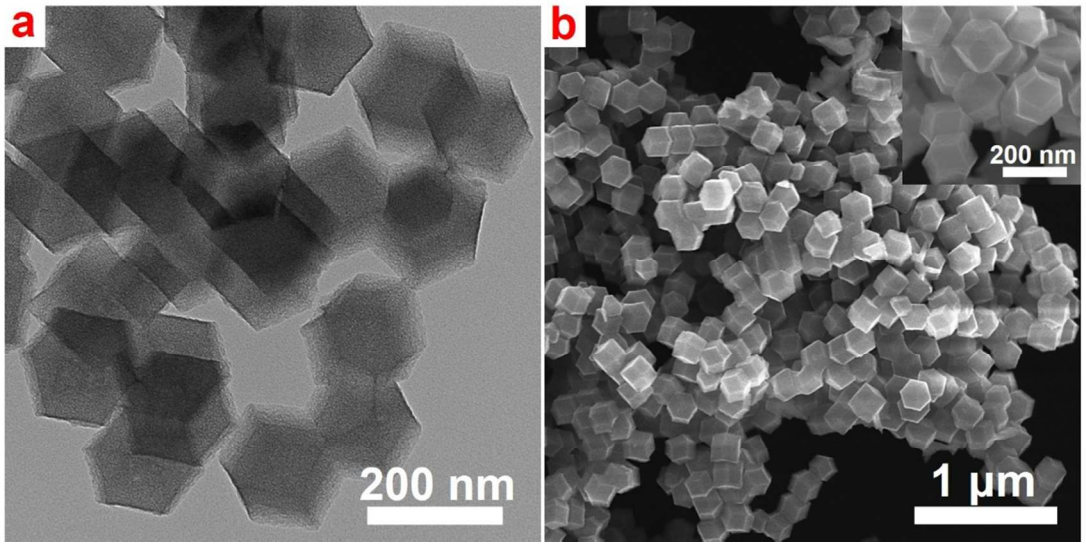

Fig. S8. (a) TEM image and (b) SEM image image of pyrolyzed Ni SAs/N-C.

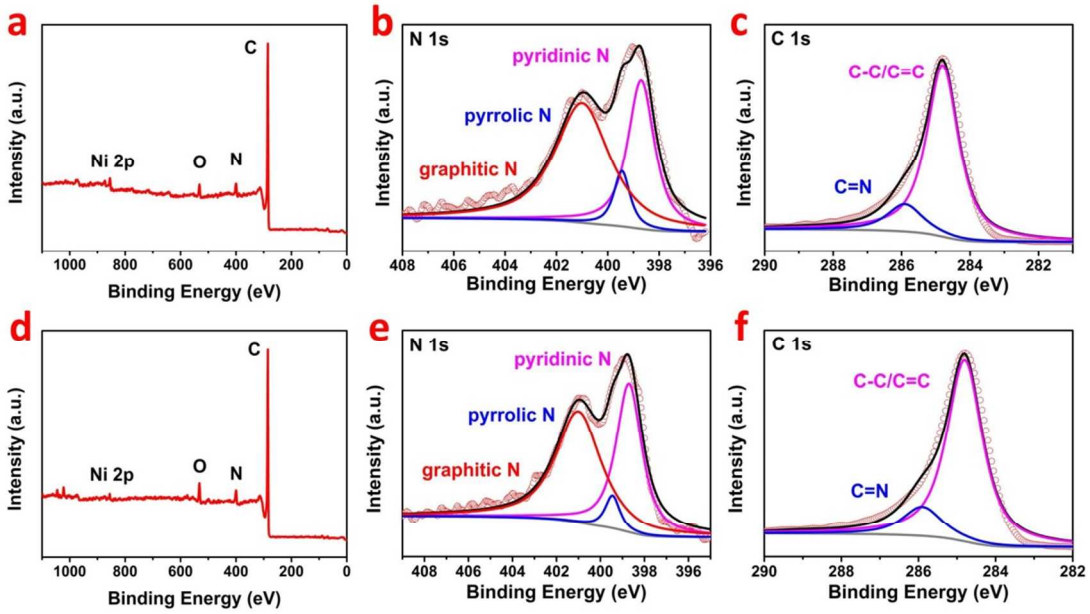

Fig. S9. XPS spectra for the (a) survey scan, (b) N 1s, (c) C 1s regions of Ni SAs/N-C. XPS spectra for the (d) survey scan, (e) N 1s, (f) C 1s regions of Ni NPs/N-C.

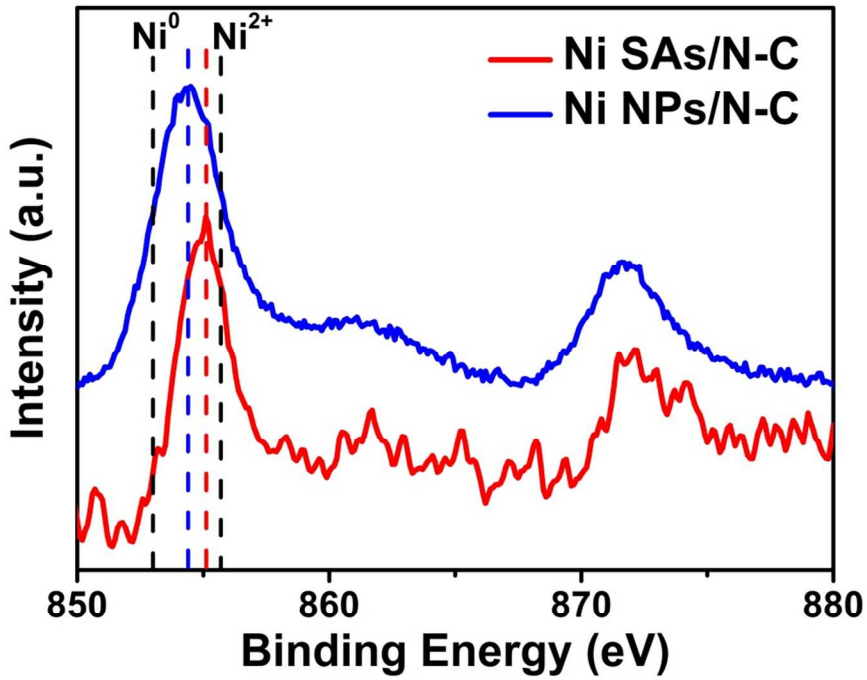

Fig. S10. XPS spectra for the Ni 2p regions of Ni SAs/N-C and Ni NPs/N-C.

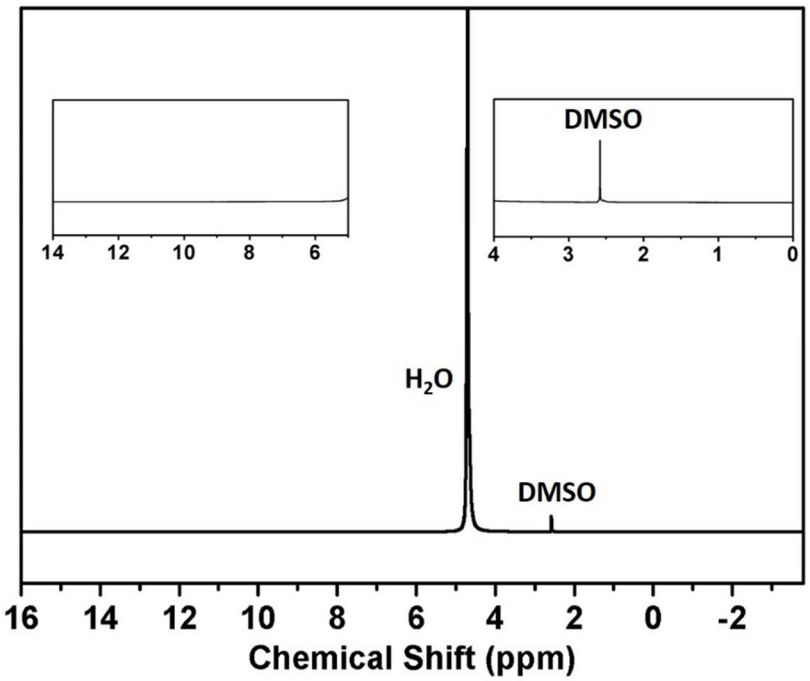

Fig. S11. Representative NMR spectra of the electrolyte after CO_2 reduction electrolysis 3h at −1.0 V versus RHE for the Ni SAs/N-C.

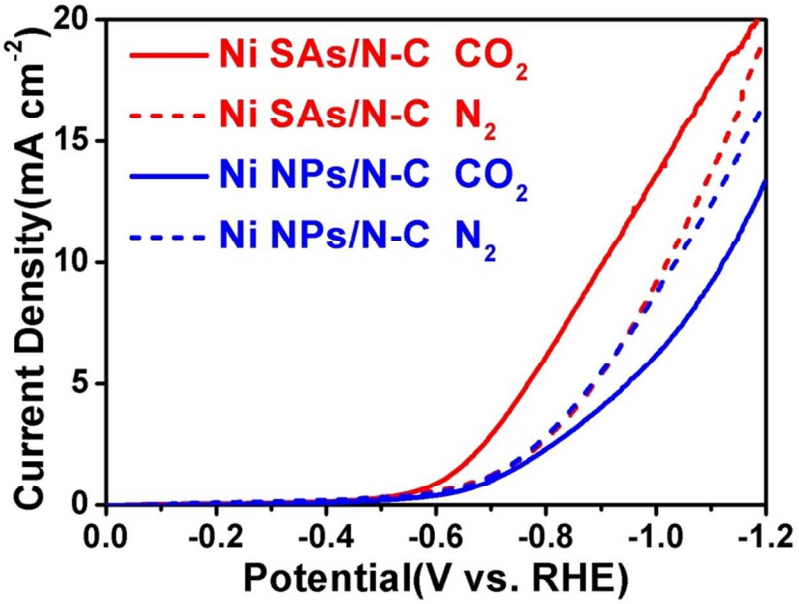

Figure S12. The LSV curves in N_2-saturated 0.5 M $NaClO_4$ solution (dotted line) and CO_2-saturated 0.5 M $KHCO_3$ (solid line) of Ni SAs/N-C and Ni NPs/N-C.

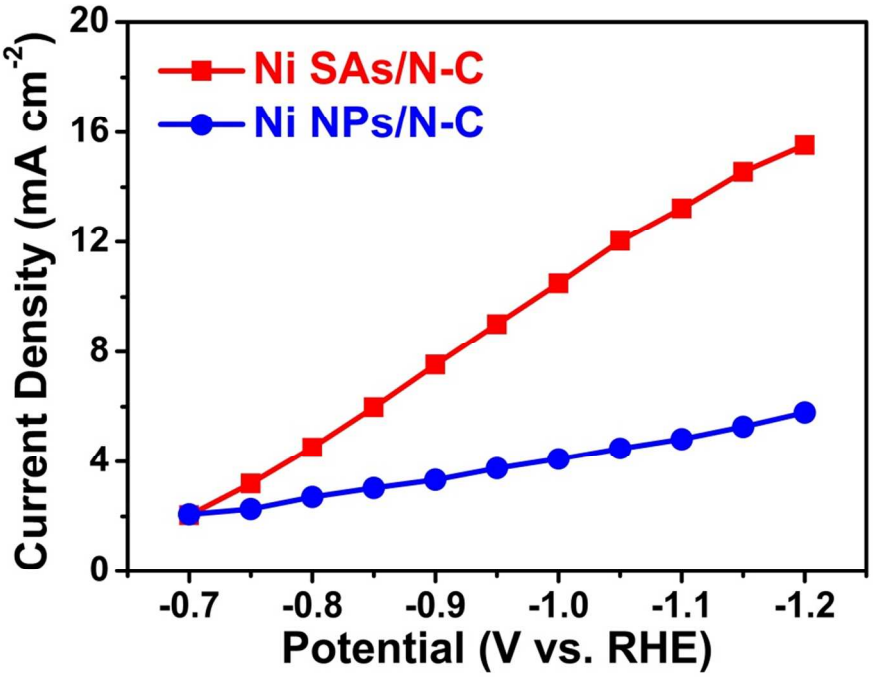

Fig S13. Total current density (based on geometric surface area) plots of the Ni SAs/N-C and Ni NPs/N-C at different applied potentials.

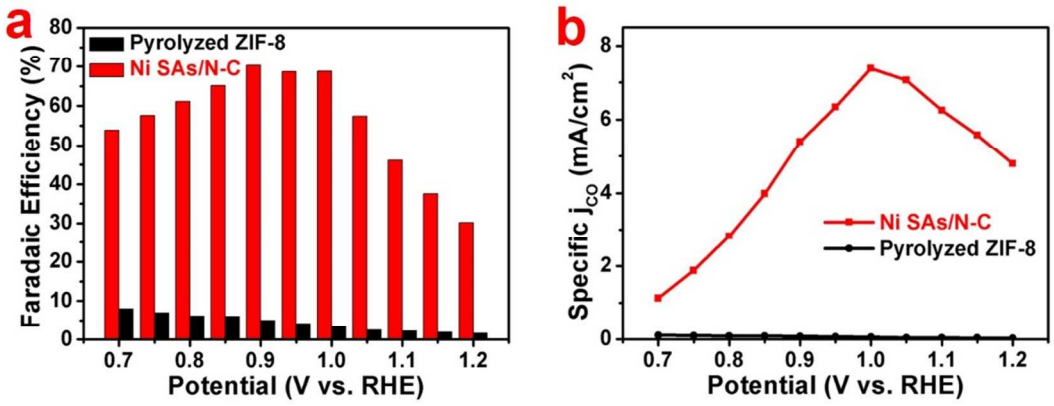

Fig. S14. The comparisons between the Ni SAs/N-C and pyrolyzed ZIF-8 at different applied potentials: (a) FE of CO and (b) Partial CO current density (based on geometric surface area).

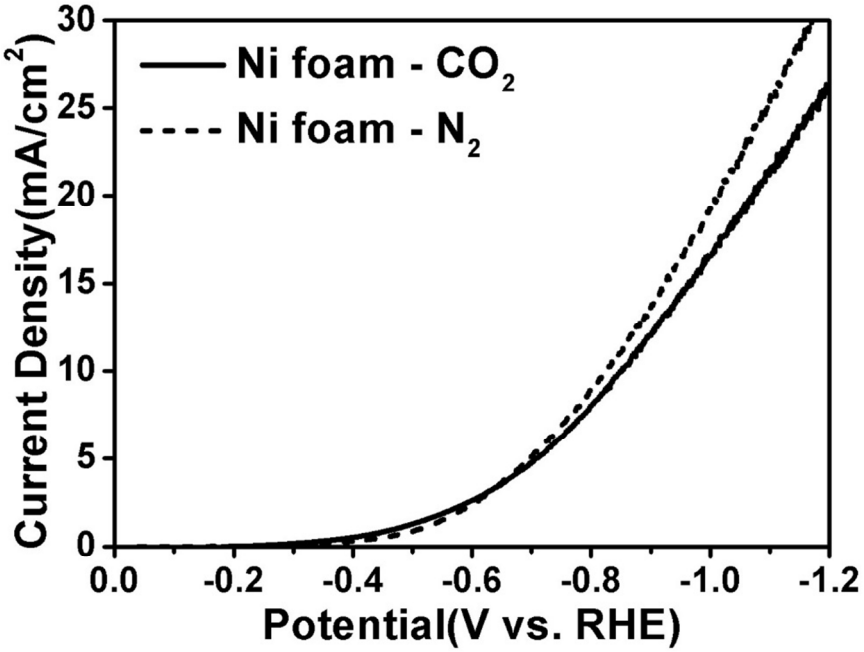

Fig. S15. LSV curves of the Ni foam at different applied potentials.

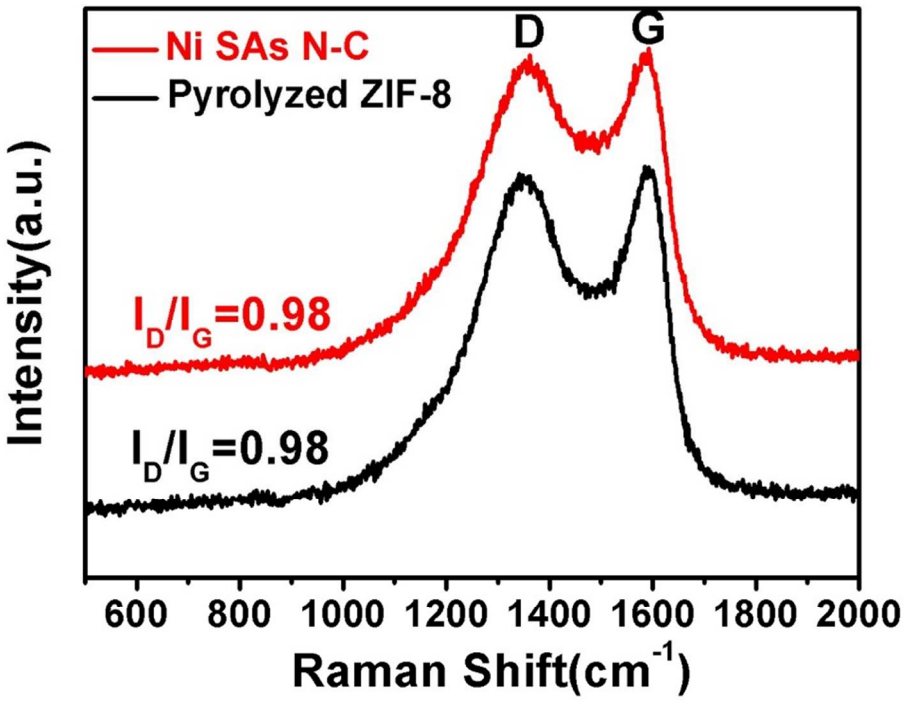

Fig. S16. Raman spectra for Ni SAs/N-C and pyrolyzed ZIF-8.

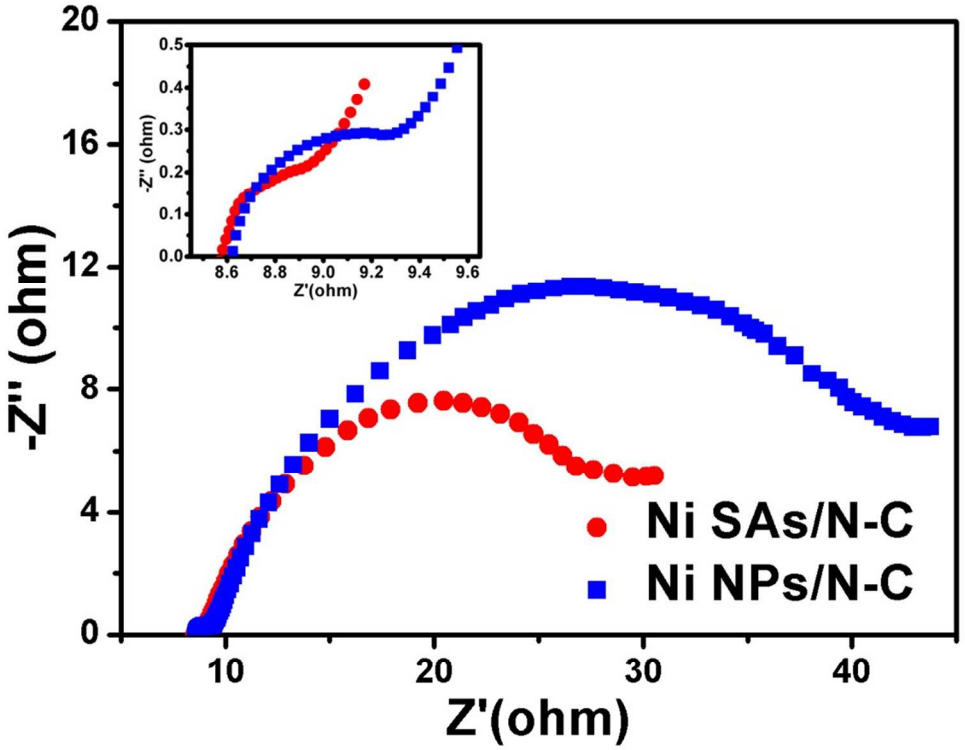

Fig. S17. Nyquist plots for Ni SAs/N-C and Ni NPs/N-C.

Table S1. EXAFS data fitting results of Ni SAs/N-C.

Sample	Scattering pair	CN	R(Å)	$\sigma^2(10^{-3}Å^2)$	ΔE_0(eV)	R factor
Ni SAs/N-C	Ni-C	0.8±0.4	1.78±0.02	4.2±0.5	-7.4±5.0	0.0031
	Ni-N	3.2±0.6	1.88±0.02	4.6±0.6		

CN, coordination number; R, interatomic distance; Debye-Waller factor; ΔE_0, edge-energy shift.

Table S2. Comparison of turnover frequency (TOFs) of various catalysts for CO_2 electroreduction.

Catalysts	Main Product	Potential Overpotential (vs. RHE)	TOF (h^{-1})	Medium and Cathode Material	Current density (mA cm^{-2})	Ref.
Ni SAs/N-C	**CO(70.3%)**	**-1.0 V (890 mV)**	**5273**	**0.5 M $KHCO_3$ Carbon paper**	**10.48**	**This work**
Au Nanowires	CO(94%)	-0.35 V (240 mV)	72	0.5 M $KHCO_3$ Carbon paper	8.16	**2**
Nanoporous Ag	CO(92%)	-0.5 V (390 mV)	7.2	0.5 M $KHCO_3$ Carbon paper	~8.7	**3**
Pd Nanoparticles	CO(91%)	-0.89 V (790 mV)	576	0.1 M $KHCO_3$ Carbon paper	~9.76	**4**

N-based silver catalyst	CO(90%)	-1.6 V (unadjusted)	ca.2000[#]	1 M KOH Carbon paper	90	**5**
Fe porphyrin	CO(94%)	-1.16 V (unadjusted) (470 mV)	11 (1.1e6*)	DMF + H_2O (2 M) Graphite crucible	0.31	**6**
COF-367-Co	CO(91%)	-0.67 V (560 mV)	165 (1908*)	0.5 M $KHCO_3$ Carbon paper	3.3	**7**
COF-367-Co(1%)	CO(53%)	-0.67 V (560 mV)	764 (9360*)	0.5 M $KHCO_3$ Carbon paper	0.45	**7**
$Al_2(OH)_2TCPP$-Co	CO(76%)	-0.7 V (560 mV)	~200	0.5 M $KHCO_3$ Carbon disk electrode	~1.0	**8**
Perfluorinated CoPc	CO(93%)	-0.8 V (690 mV)	5760	0.5 M $KHCO_3$ Carbon cloth	~4.4	**9**
CAT_{Pyr}/CNT	CO(93%)	-0.59 V (480 mV)	144	0.5 M $KHCO_3$ Glassy carbon electrode	0.24	**10**

Calculated on the basis of the amount of bulk catalytic material deposited on the electrode surface.

* Calculated on the basis of the amount of electroactive sites on the electrode surface.

The following equation is used to estimate TOF: $TOF = QE_F/(tNFn_{cat}) = iE_{F/}(NFn_{cat})$, where Q is the total charge passed in time t, i is the current, E_F is the Faradaic efficiency for the desired product, N is the number of electrons in the half reaction (N = 2 for CO_2 to CO or HCO_2H conversion), and F is the Faraday constant (F = 96485 C/mol electrons).

For TOF values based on electroactive catalytic sites using various different methods, please see the corresponding reference.

4. References

(1) Yang, J.; Zhang, F.; Lu, H.; Hong, X.; Jiang, H.; Wu, Y.; Li, Y. *Angew. Chem., Int. Ed.* **2015***, 54,* 10889.

(2) Zhu, W.; Zhang, Y. J.; Zhang, H.; Lv, H.; Li, Q.; Michalsky, R.; Peterson, A. A.; Sun, S. *J. Am. Chem. Soc.* **2014***, 136,* 16132.

(3) Lu, Q.; Rosen, J.; Zhou, Y.; Hutchings, G. S.; Kimmel, Y. C.; Chen, J. G.; Jiao, F. *Nat. Commun.* **2014***, 5,* 3242.

(4) Gao, D.; Zhou, H.; Wang, J.; Miao, S.; Yang, F.; Wang, G.; Wang, J.; Bao, X. *J. Am. Chem. Soc.* **2015***, 137*, 4288.

(5) Tornow, C. E.; Thorson, M. R.; Ma, S.; Gewirth, A. A.; Kenis, P. J. *J. Am. Chem. Soc.* **2012***, 134*, 19520.

(6) Costentin, C.; Drouet, S.; Robert, M.; Savéant, J.-M. *Science* **2012***, 338,* 90.

(7) Lin, S.; Diercks, C. S.; Zhang, Y.-B.; Kornienko, N.; Nichols, E. M.; Zhao, Y.; Paris, A. R.; Kim, D.; Yang, P.; Yaghi, O. M. *Science* **2015***, 349,* 1208.

(8) Kornienko, N.; Zhao, Y.; Kley, C. S.; Zhu, C.; Kim, D.; Lin, S.; Chang, C. J.; Yaghi, O. M.; Yang, P. *J. Am. Chem. Soc.* **2015***, 137,* 14129.

(9) Morlanés, N.; Takanabe, K.; Rodionov, V. *ACS Catal.* **2016***, 6,* 3092.

(10) Maurin, A.; Robert, M. *J. Am. Chem. Soc.* **2016***, 138,* 2492.